NIH Public Access
Author Manuscript
Neuroimage. Author manuscript; available in PMC 2012 January 1.

Published in final edited form as:
Neuroimage. 2011 January ; 54S1: S196–S203. doi:10.1016/j.neuroimage.2009.08.069.

Optimal Region of the Putamen for Image-Guided Convection-Enhanced Delivery of Therapeutics in Human and Non-human Primates

Dali Yin, MD, PhD., **Francisco E. Valles, BS**, **Massimo S. Fiandaca, MD**, **John Bringas, BS**, **Francisco Gimenez**, **Mitchel S. Berger, MD**, **John Forsayeth, PhD**, and **Krystof S. Bankiewicz, MD, PhD***
Department of Neurosurgery, University of California San Francisco, 1855 Folsom Street, San Francisco, CA 94103

Abstract

Optimal results in the direct brain delivery of brain therapeutics such as growth factors or viral vector into primate brain depends on reproducible distribution throughout the target region. In the present study, we retrospectively analyzed MRI of 25 convection-enhanced delivery (CED) infusions with MRI contrast into the putamen of non-human primates (NHP). Infused volume (Vi) was compared to total volume of distribution (Vd), vs. Vd within the target putamen. Excellent distribution of contrast agent within the putamen was obtained in 8 cases that were used to define an optimal target volume, or “green” zone. Partial or poor distribution with leakage into adjacent anatomical structures was noted in 17 cases, defining “blue” and “red” zones respectively. Quantitative containment (99 ± 1%) of infused Gadoteridol within the putamen was obtained when the cannula was placed in the green zone, 87 ± 3% in the blue zone and 49 ± 0.05% in the red zone. These results were used to determine a set of 3D stereotactic coordinates that define an optimal site for putaminal infusions in NHP and human putamen. We conclude that cannula placement and definition of optimal (green zone) stereotactic coordinates have important implications in ensuring effective delivery of therapeutics into the putamen utilizing routine stereotactic MRI localization procedures, and should be considered when local therapies such as gene transfer or protein administration are being translated into clinical therapy.

Keywords

MRI; Parkinson’s disease; convection-enhanced delivery; cannula placement; non-human primate

Introduction

Convection-enhanced delivery (CED) is an interstitial central nervous system (CNS) delivery technique (Bobo et al., 1994) that also circumvents the blood-brain barrier in delivering agents into the central nervous system (CNS). Traditional local delivery of most

*Corresponding Author and Reprint Requests: Krystof S. Bankiewicz, Department of Neurosurgery, University of California San Francisco, 1855 Folsom Street, MCB 226, San Francisco, CA 94103. Tel: (415) 502-3132; Fax: (415) 514-2864. Krystof.Bankiewicz@ucsf.edu.

Publisher's Disclaimer: This is a PDF file of an unedited manuscript that has been accepted for publication. As a service to our customers we are providing this early version of the manuscript. The manuscript will undergo copyediting, typesetting, and review of the resulting proof before it is published in its final citable form. Please note that during the production process errors may be discovered which could affect the content, and all legal disclaimers that apply to the journal pertain.

NIH-PA Author Manuscript
NIH-PA Author Manuscript
NIH-PA Author Manuscript

NIH-PA Author Manuscript

NIH-PA Author Manuscript

NIH-PA Author Manuscript

therapeutic agents into the brain has relied on diffusion, which depends on a concentration gradient. The rate of diffusion is inversely proportional to the size of the agent, and is usually slow with respect to tissue clearance. Thus, diffusion results in a non-homogeneous distribution of most delivered agents and is restricted to a few millimeters from the source. In contrast, CED uses a fluid pressure gradient established at the tip of an infusion catheter and bulk flow to propagate substances within the extracellular fluid space (Bobo et al., 1994). CED allows the extracellularly-infused material to further propagate via the perivascular spaces and the rhythmic contractions of blood vessels acting as an efficient motive force for the infusate (Hadaczek et al., 2006b). As a result, a higher concentration of drug is distributed more evenly over a larger area of targeted tissue than would be seen with a simple injection. Currently, CED has been clinically tested in the fields of neurodegenerative diseases, such as Parkinson's disease (PD) (Eberling et al., 2008; Gill et al., 2003), and neuro-oncology (Kunwar, 2003; Mardor et al., 2001). Laboratory investigations with CED cover a broad field of application, such as the delivery of small molecules (Carson et al., 2002) (Lonser et al., 1999), macromolecules (Bobo et al., 1994), viral particles (Richardson et al., 2008), magnetic nanoparticles (Kroll et al., 1996), and liposomes (Krauze et al., 2006).

PD is characterized by progressive loss of dopaminergic neurons in the substantia nigra and a severe decrease of dopamine within the striatum (Hornykiewicz, 1975), and the putamen is a primary site for the principal neuropathology associated with the disorder (Aminoff, 2001). For this reason, our group has used the putamen as the primary target for enzyme replacement gene therapy delivered via CED for PD (Bankiewicz et al., 2006; Bankiewicz et al., 2000; Eberling et al., 2008; Forsayeth et al., 2006). Other groups have also targeted the putamen with growth factors, either as recombinant protein (Lang et al., 2006) or in a gene therapy vector (Gasmi et al., 2007; Herzog et al., 2007). One reason that these studies were unsuccessful may have been that distribution of the therapeutic agent within the putamen was poorly controlled.

CED visualization with the aid of novel contrast materials co-infused with therapeutic agents has recently been investigated in rodent (Saito et al., 2004), non-human primates (NHP) (Lonser et al., 2002; Murad et al., 2007; Saito et al., 2005) and humans (Lonser et al., 2007) (Sampson et al., 2006). We have used real-time MRI to visualize the CED process with the aid of Gadoteridol-loaded liposomes (GDL) that co-distribute with the therapeutic being delivered to the putamen of NHP (Krauze et al., 2005a; Saito et al., 2005). During CED, the volume of distribution (Vd) for a given agent depends on the structural properties of the tissue being convected (Fiandaca et al., 2008b), such as hydraulic conductivity, vascular volume fraction, and extracellular fluid fraction. It also depends on the technical parameters of the infusion procedure such as cannula design, cannula placement, infusion volume, and rate of infusion, with the overall aim of improving delivery efficiency while attempting to limit the spread of the therapeutic into regions outside the target. In our experience, a key component of successful CED for PD patients is likely to be the site of cannula placement within the putamen. Selection of the optimal cannula type for effective CED delivery in the brain is also critical. We examined several types of cannulae with respect to size and design and concluded that a stepped design with a fused silica tip provided us with the most consistently robust brain delivery (Krauze et al., 2005c; Sanftner et al., 2005). The stepped cannula dramatically reduces reflux along the infusion device by restricting initial backflow of fluid flow beyond the step. To obtain effective distribution of the infused therapeutic within the putamen, it is essential to understand the optimal site of placement of the step and tip of the infusion cannula within that target and surrounding white matter tracts that serve as leakage points (Varenika et al., 2008). Such an understanding may allow precise delivery of the therapeutic to the target structure(s), while lessening the risk of leakage to surrounding brain structures. The current work was designed,

NIH-PA Author Manuscript

NIH-PA Author Manuscript

NIH-PA Author Manuscript

therefore, to establish parameters that could help define the area for cannula step placement in order to obtain optimal distribution of therapeutic agents within the putamen in the upcoming CED-based studies in PD patients. This study may also explain some of the failures of CED, in both NHP studies and human clinical trials, that may have been related to suboptimal targeting of infusion cannula.

Materials and Methods

Experimental subjects and study design

Thirteen normal adult NHP, including 11 Rhesus macaques (7 male and 4 female, aged from 8 to 18 years; mean age 11.9 years, weight 4 – 9.4 kg) and 2 Cynomolgus monkeys (one male and one female, age 7 years for both; weight 5 and 7 kg respectively) were the subjects in the present study. Experimentation was performed according to the National Institutes of Health guidelines and to the protocols approved by the Institutional Animal Care and Use Committee at the University of California San Francisco (San Francisco, CA) and at Valley Biosystems (Sacramento, CA). The thirteen animals received a total of 25 intracranial infusion of GDL (2 mM Gd-DTPA) or free Gadoteridol (2 mM Gd-DTPA, Prohance; Bracco Diagnostics, Princeton, NJ) into the putamen. GDL gives stronger contrast than free Gadoteridol, but the distribution characteristics are otherwise identical (manuscript in preparation). Infusions were performed by previously established CED techniques for NHP (Bankiewicz et al., 2000). GDL were prepared as previously described (Fiandaca et al., 2008a; Krauze et al., 2005a).

Infusion procedure

Primates received a baseline MRI before surgery to visualize anatomical landmarks and to generate stereotactic coordinates of the proposed target infusion sites for each animals. NHP underwent neurosurgical procedures to position the MRI-compatible guide cannula over the putamen. Each customized guide cannula was cut to a specified length, stereotactically guided to its target through a burr-hole created in the skull, and secured to the skull by dental acrylic. The larger diameter stem of the cannula had an outer and inner diameter of 0.53 mm and 0.45 mm respectively. The outer and inner diameters of the tip segment were 0.436 and 0.324 mm respectively. The tops of the guide cannula assemblies were capped with stylet screws for simple access during the infusion procedure. Animals recovered for at least 2 weeks before initiation of infusion procedures. Animals were anesthetized with isoflurane (Aerrane; Ohmeda Pharmaceutical Products Division, Liberty Corner, NJ) during real-time MRI acquisition. Each animal's head was placed in an MRI-compatible stereotactic frame, and a baseline MRI was performed. Vital signs, such as heart rate and PO_2, were monitored throughout the procedure. Briefly, the infusion system consisted of a fused silica reflux-resistant cannula (Fiandaca et al., 2008a; Krauze et al., 2005a) that was connected to a loading line (containing GDL or free Gadoteridol), an infusion line with oil, and another infusion line with trypan blue solution. A 1-ml syringe (filled trypan blue solution) mounted onto a micro-infusion pump (BeeHive, Bioanalytical System, West Lafayette, IN), regulated the flow of fluid through the system. Based on MRI coordinates, the cannula was mounted onto a stereotactic holder and manually guided to the targeted region of the brain through the previously placed guide cannula. The length of each infusion cannula was measured to ensure that the distal tip extended 3 mm beyond the length of the respective guide. This created a stepped design at the tip of the cannula to maximize fluid distribution during CED procedures and minimize reflux along the cannula tract. In the text, we refer to this transition from fused silica tip to a fused silica sheath as the "step", and all positioning data is derived from the position of this step because of its unambiguous visibility on MRI. After securing placement of the infusion cannula, the CED procedures were initiated with real-time MRI data being acquired (real-time convective delivery, RCD).

NIH-PA Author Manuscript

NIH-PA Author Manuscript

NIH-PA Author Manuscript

We used the same infusion parameters for every NHP infused throughout the study. Infusion rates were as follows: 0.1 μl/min was applied when lowering cannula to targeted area and increased at 10-min intervals to 0.2, 0.5, 0.8, 1.0, and 2.0 μl/min. Approximately 15 min after infusion, the cannula was withdrawn from the brain. Four animals received multiple infusions. Each animal had at least a 4-week interval between each infusion procedure.

Magnetic resonance image (MRI)

NHP were sedated with a mixture of ketamine (Ketaset, 7 mg/kg, IM) and xylazine (Rompun, 3 mg/kg, IM). After sedation, each animal was placed in a MRI-compatible stereotactic frame. The ear-bar and eye-bar measurements were recorded, and an intravenous line was established. MRI data was then obtained, after which animals were allowed to recover under close observation until able to right themselves in their home cages. MR images of brain in 9 NHP were acquired on a 1.5T Siemens Magnetom Avanto (Siemens AG, Munich, Germany). Three-dimensional rapid gradient echo (MP-RAGE) images were obtained with repetition time (TR) = 2110 ms, echo time (TE) = 3.6 ms, and a flip angle of 15°, number of excitations (NEX) = 1 (repeated 3 times), matrix = 240 × 240, field of view (FOV) = 240 × 240 × 240, and slice thickness = 1 mm. These parameters resulted in a 1-mm^3 voxel volume. The scanning time was approximately 9 min. MR images in 4 NHP were acquired on a 1.5-T Sigma LX scanner (GE Medical Systems, Waukesha, WI) with a 5-inch surface coil on the subject's head, parallel to the floor. Spoiled gradient echo (SPGR) images were T1-weighted and obtained with a spoiled grass sequence, a TR = 2170 ms, a TE = 3.8 ms, and a flip angle of 15°. The NEX = 4, matrix = 256 × 192, FOV = 16 cm × 12 cm, slice thickness = 1 mm. These parameters resulted in a 0.391 mm^3 voxel volume. Scanning time was approximately 11 min.

Volume and distance measurements in NHP brain

MR images were obtained from each real-time convective delivery (RCD), and used to measure distance from cannula step to corpus callosum (CC), internal capsule (IC) and external capsule (EC). The measurements were made on an Apple Macintosh G4 computer with OsiriX® Medical Image Software (v2.5.1). OsiriX software reads all data specifications from DICOM (digital imaging and communications in medicine) formatted MR images obtained via local picture archiving and communication system (PACS). For each image, the default window and level settings were used throughout the study; that is, there was no attempt to alter or manipulate settings from one experiment to another. The distances from cannula step to each above-mentioned structure were manually defined, and then calculated by the software. All the distances were measured in the same manner on MRI sections.

The X, Y and Z axial values of cannula step location in green zone were determined with 2D orthogonal MR images generated by OsiriX software, where MR images were projected in all three dimensions (axial, coronal and sagittal). We used midpoint of the anterior commissure-posterior commissure (AC-PC) line as zero point (0,0,0) of three-dimensional (3D) brain space. Briefly, AC-PC line was drawn on mid-sagittal plane of MRI, and the midpoint of AC-PC line was determined. The horizontal and vertical plane through the midpoint of AC-PC line was then obtained, and they could be shown on all the three plans simultaneously. The X, Y and Z axial values of cannula step were then obtained by measurements of distance from cannula step to midline on coronal MRI plane (X value), distance anterior (or posterior) to the midpoint of AC-PC line of the coronal MRI plane (Y value), and the distance above (or below) axial plane incorporating the AC-PC line on MRI (Z value). All the distances were measured (in millimeters) in the same manner on MRI sections for each case.

NIH-PA Author Manuscript

NIH-PA Author Manuscript

NIH-PA Author Manuscript

MR images were also used for volumetric quantification of distribution of Gadoteridol. The Vd of Gadoteridol in the brain of each subject was also quantified on an Apple Macintosh G4 computer. ROI derived in the putamen and white matter track were manually defined, and software then calculated the area from each MR image, and established the volume of the ROI, based on area defined multiplied by slice thickness (PACS volume). The boundaries of each distribution were defined in the same manner in the series of MRI sections. The sum of the PACS ROI volumes (number of MRI slices evaluated) for the particular distribution being analyzed determined the measured structure volume. The defined ROI volumes allowed for 3D image reconstruction with BrainLAB software (BrainLAB, Heimstetten, Germany). MRIs were evaluated and all measurements performed by two independent observers blind to each other. In a preliminary comparison of distances measured by the two observers in NHP, there was no significant difference between the mean values obtained.

Statistical Analysis

The distance from cannula step to corpus callosum, internal capsule and external capsule obtained when the step was located in different zones were compared across subject groups by Student's t-test. The criterion for statistical significance for all tests was $p < 0.05$.

Results

In this study, thirteen NHP received twenty-five putaminal infusions. Real-time MR images of NHP brain were obtained from each RCD to evaluate the distribution of Gadoteridol, and to measure the distance from step of cannula in the putamen to CC, IC and EC based on the location of the cannula step. We observed that some infusions resulted in poor containment of tracer within putamen with significant distribution into adjacent white matter tracts (WMT) of the corpus callosum (CC) and occasionally internal (IC) and external (EC) capsules, whereas others distributed tracer only into putamen (Table 1). When the percent of infused tracer contained within the putamen was plotted against each variable (Fig. 1), it was apparent that reflux along the cannula correlated (Fig. 1A) with a sharp decline in distribution of infusate into the putamen (PUT). This finding was further emphasized by the decline in Vd/Vi ratios as extra-putaminal distribution became more evident. The mean ratio when infusate was well-contained within putamen was 6.65 ± 0.51. However, infusions in which some leakage was observed evinced a ratio of 4.60 ± 0.25, falling to only 2.92 ± 0.37 for infusions in which considerable leakage was observed. We interpret this decline to signify inhibition of distribution into the target putamen even as further increases in infusate volume are applied. This finding is in agreement with previous studies showing that the appearance of significant leakage or reflux during an infusion strongly inhibits further increases in Vd (Varenika et al., 2008). Containment of tracer within putamen (PUT) in excess of 95% is achievable with backflows of less than about 5 mm. The tip length in these experiments was 3 mm.

Subsequent correlations between PUT coverage and anatomical coordinates revealed also that another key variable appears to be the distance from the corpus callosum (CC) to the cannula step (Fig. 1B). In 8 infusions in which putaminal containment exceeded 95%, the cannula step-to-CC ranged from 3.14 mm to 3.76 mm with mean distance of 3.35 ± 0.08 mm, the step-to-IC ranged from 2.13 mm to 5.65 mm with mean distance of 4.01 ± 0.42 mm, and the step-to-EC ranged from 1.98 mm to 3.28 mm with mean distance of 2.75 ± 0.17 mm. We conclude that the step-to-CC distance should exceed about 3 mm for optimal containment of infusate within putamen. The distance from the cannula step to IC and EC (Fig. 1C, D) correlated poorly with putaminal containment. We defined the spatial limits associated with essentially quantitative putaminal containment of tracer as the "green zone".

NIH-PA Author Manuscript

NIH-PA Author Manuscript

NIH-PA Author Manuscript

A corresponding “blue zone”, associated with putaminal containment of tracer in from 79% to 94% with mean of 87 ± 3% indicative of a small amount of leakage into the CC, was also defined in 4 cases. Here the step-to-CC ranged between 2.74 mm and 2.88 mm with mean distance of 2.81 ± 0.04 mm; the step-to-IC ranged from 3.26 mm to 4.86 mm with mean distance of 4.18 ± 0.37 mm, and the step-to-EC from 1.92 mm to 3.43 mm with mean distance of 2.68 ± 0.36 mm.

Similarly, a “red zone” was defined in 13 cases where tracer was poorly confined to PUT, ranging from 31% to 67% of PUT with a mean of 49 ± 0.05%, indicating a large amount of leakage into the CC, EC and IC. In these infusions, the step-to-CC ranged from 0.12 mm to 1.99 mm with mean distance of 1.26 ± 0.16 mm; the step-to-IC ranged from 0.65 mm to 4.08 mm with mean distance of 2.63 ± 0.27 mm, and the step-to-EC from 0.85 mm to 4.25 mm with mean distance of 1.88 ± 0.25 mm.

Volume of distribution of Gadoteridol in the brain

When the step was placed in the “green zone” in 8 cases, excellent Vd of Gadoteridol was obtained in the putamen, ranging from 52.9 to 174.1 mm^3 with mean volume of 116.4 ± 0.04 mm^3 (Fig. 2A, B). Two cases were found to have minor leakage of Gadoteridol into CC at the end of infusion, with Vd in white matter tract (WMT) of 2.7 and 6.1 mm^3 (Fig. 2C, F).

In 4 cases in which the step was placed in the blue zone, the Vd of Gadoteridol in the putamen ranged from 40.7 to 261.9 mm^3 with mean volume of 139.6 ± 0.05 mm^3 (Fig. 2A, B). All 4 cases were found to have leakage into CC. When leakage was first seen, the infusion volume ranged from 4.7 to 10.5 μl with mean volume of 6.9 ± 0.9 μl. The final Vd in WMT ranged from 6.3 to 40.7 mm^3 with mean volume of 19.4 ± 0.01 mm^3 (Fig. 2D, G).

Placement of the step in the “red zone” in 13 cases produced a Vd of Gadoteridol from 17.7 to 97.5 mm^3 with mean volume of 62.1 ± 0.01 mm^3 (Fig. 2A, B). All 13 cases were found to have considerable leakage into CC with variable leakage into IC and EC. When leakage was first seen, the infusion volume was between 1.6 and 21.8 μl with mean volume of 7.9 ± 1.7 μl. The final Vd in WMT ranged from 26.7 to 152.2 mm^3 with a mean volume of 66.8 ± 0.01 mm^3. Of 17 cases with relatively large leakage during CED, leakage into CC was found in all 17 cases (100%), into IC in 3 cases (17.6%) and into EC in one case (5.9%) (Fig. 2E, H).

Coordinates for green zone in the putamen of 3D brain space in NHP

The midpoint of the AC-PC line was defined as the zero point (0,0,0) of a 3D brain space. Based on the coordinate calculations for the cannula step by MRI, the target for green zone in the putamen ranged from 9.57 to 14.95 mm with mean distance of 11.85 ± 0.56 mm lateral (X coordinate), from 5.88 to 8.93 mm with mean distance of 7.36 ± 0.49 mm anterior to the of AC-PC midpoint (Y coordinate), and from 1.64 to 4.47 mm with mean distance of 3.62 ± 0.40 mm superior to the AC-PC axial plane (Z coordinate).

RGB zones for cannula step in the putamen of NHP

On the basis of these analyses, we have defined coordinates for putaminal infusions that identify preferred cannula characteristics and optimal distances from major structures in the brain (RGB zones). The “green zone” is defined as a volume at least 3 mm ventral to the CC, at least 6 mm away from the AC (3 mm from cannula tip to AC plus 3 mm of tip length) vertically, greater than 2.75 mm from EC laterally, and more than 3 mm from IC medially. If globus pallidus is included, then the optimal distance from IC is more than 4.01 mm. The “blue zone” is defined as a thick shell surrounding the “green zone” of which the outer border of “blue zone” is approximately 0.5 mm from the outer edge of the green zone.

NIH-PA Author Manuscript

NIH-PA Author Manuscript

NIH-PA Author Manuscript

Finally, the “red zone” is defined as the area from the outer border of the blue zone to the margin of the putamen. Based on these parameters, RGB zones for cannula placement in the NHP putamen were defined on MRI (Fig. 3A). Next, we also outlined “green zone” only, and then calculated the volume of the green zone to be 10.3 mm^3 with an anterior-posterior length of 8.5 mm (Fig. 4A).

Containment vs. distribution in NHP putamen

In the above studies, only small amounts (<30 μl) of tracer were infused sufficient to register the relative partitioning of infusate into PUT, CC, IC, and/or EC. We wished, however, to show that infusion of larger volumes into green zone would faithfully distribute into PUT with no untoward non-putaminal distribution. By retrospective examination of other putaminal infusions in NHP, we found that in animals where cannula placement was in the green zone, excellent containment of infusate within PUT was seen at small (< 30 μl) and large (> 100 μl) volumes (Fig. 5). In contrast, cannula placement in blue zone was associated with increasing distribution of infusate into WMT as the volume of infusion grew. These representative data confirmed that, with a defined RGB zone system in hand, we could identify optimal infusions on the basis of optimal cannula placement alone.

RGB zones in the putamen of human brain

We used the parameters for RGB zone obtained from NHP to predict RGB zones in the putamen of human brain (Fig. 3B). We understand that the predicted RGB zone in human putamen is still uncertain, and further clinical study will be done to confirm this prediction. However, it may serve as an approximate guide to RGB zones in human PUT when local therapies such as gene transfer or protein administration are translated into clinical therapy. We also outlined the green zone on serial MR images and then calculated the area from each MR image to predict that the volume of the green zone is 239.5 mm^3 with an anterior-posterior distance of 19.7 mm (Fig. 4B). The RGB zones for cannula step in the PUT of NHP and human are also compared as shown in Fig. 3 on the same scale.

Discussion

In the present study, we correlated the precise stereotactic placement of the infusion cannula in PUT of NHP with the efficiency of MRI tracer distribution into the PUT. Clearly, some infusions were associated with excellent containment of tracer, others were somewhat less efficient and displayed some evidence of reflux. A number of infusions, however, were poorly contained within PUT and were associated with leakage of tracer primarily into corpus callosum WMT. Analysis of these data (Fig. 1) indicated that the variables most determinant of putaminal containment were the length of the cannula tip and the distance of the cannula step to the corpus callosum. Distance of the step to the internal and external capsules correlated poorly with containment. The correlation between stereotactic coordinates of the cannula and resulting PUT:WMT partition of tracer permitted us to define a putaminal “green zone”, a 3D space in which cannula placement is optimal and convection of infusate into putamen is optimal. Similarly, a “blue zone” was defined as sub-optimal but still acceptable in some cases, and a “red zone” associated with unacceptable results. In addition, we showed that the “green zone” predicts effective Vd into PUT where untoward leakage of infusate into WMT may be avoided. Reflux up the cannula track cause a disruption of the pressure gradient which compromises distribution of the infusate in the PUT, leading to reduced Vd. Leak of the infusate into the CC is most common and it depends on proximity of the step to CC, as we show in this report. If the step is close to CC, combined with the fact that the cannula axis runs through it, reflux will always occurs in the direction of the cannula axis.

NIH-PA Author Manuscript

NIH-PA Author Manuscript

NIH-PA Author Manuscript

We used the NHP “green zone” to predict a corresponding zone in human PUT. Our computational analysis suggested that human has a proportionately larger green zone compared with NHP, and that the 23-fold difference in volume of green zone is due to the size difference between NHP and human PUT as shown previously (Yin et al., 2009). Apart from the obvious difference in size, the overall morphology of the green zone is remarkably similar. This knowledge is critical in obtaining excellent Vd of therapeutics in the putamen of patients without significant leakage into surrounding anatomical structures.

With the more widespread use of CED in the treatment of human neurological diseases, as has be previously described (Eberling, et al 2008, Gill et al, 2003, Kunwar 2003, Mardor et al, 2001), controlled distribution of therapeutic agents within brain structures is essential for any approach utilizing gene or molecular therapy. It is important for optimizing efficacy to cover the entire targeted treatment volume while avoiding adjacent regions of the brain or CSF pathways. It has been very difficult to predict the distribution of therapeutics delivered by CED, due to a lack of understanding of optimal cannula placement under these circumstances. This is true for delivery of chemotherapeutic agents to brain tumors, and for infusion of growth factors, enzymes, and viral vectors in PD patients (Bobo et al., 1994; Hadaczek et al., 2006a; Herzog et al., 2009; Krauze et al., 2006; Krauze et al., 2005a; Krauze et al., 2005b; Saito et al., 2005).

Emergence of iMRI technology for intraoperative imaging of functional neurosurgical therapeutic interventions, such as MRI-guided placement of DBS stimulating electrodes in PD (Larson et al., 2008; Martin et al., 2009), is another example of image-guided therapy application in the brain. Precise targeting of “green zone” for CED can be accomplished by use of skull mounted aiming devices and the iMRI unit. In addition to visualization of accurate placement of the infusion cannula, desired distribution of the therapeutic agent can be achieved by visualization of the CED and subsequent control of the infusion procedure.

In summary, the present study provides the first quantitative analysis by MRI of cannula placement and distribution of Gadoteridol, and introduces the concept of RGB zones in the NHP putamen. Moreover, real-time visualization of cannula placement by MRI, and subsequent precise control of the extent of Gadoteridol distribution, addresses an important safety issue, especially when parenchymal infusion of large volumes is necessary and leakage or excessive distribution may be undesirable. Cannula placements in the RGB zones developed from our translational non-human primate studies have significant implications for the design of future clinical trials featuring CED of various therapeutic agents into the putamen for PD. Additional NHP studies and RCD infusions in human patients will need to be carried out to confirm and refine the data of RGB zones in the human putamen. It is likely that similar RGB zones can be defined for other brain regions as well, such as thalamus and brainstem, thereby establishing reliable coordinates for neurosurgical infusions of therapeutic agents in the clinic.

Acknowledgments

This work was supported by a NIH-NCI award (1 P01 CA118816-01A2) and a generous gift from the Kinetics Foundation. The authors would like to thank Drs. Paul Larson, Phillip Starr and Alastair Martin for useful discussions.

References

Aminoff MJ. Parkinson’s disease. Neurol Clin 2001;19:119–128. vi. [PubMed: 11471760]

Bankiewicz KS, Daadi M, Pivirotto P, Bringas J, Sanftner L, Cunningham J, Forsayeth JR, Eberling JL. Focal striatal dopamine may potentiate dyskinesias in parkinsonian monkeys. Exp Neurol 2006;197:363–372. [PubMed: 16337943]

NIH-PA Author Manuscript

NIH-PA Author Manuscript

NIH-PA Author Manuscript

Bankiewicz KS, Eberling JL, Kohutnicka M, Jagust W, Pivirotto P, Bringas J, Cunningham J, Budinger TF, Harvey-White J. Convection-enhanced delivery of AAV vector in parkinsonian monkeys; in vivo detection of gene expression and restoration of dopaminergic function using pro-drug approach. Exp Neurol 2000;164:2–14. [PubMed: 10877910]

Bobo RH, Laske DW, Akbasak A, Morrison PF, Dedrick RL, Oldfield EH. Convection-enhanced delivery of macromolecules in the brain. Proc Natl Acad Sci U S A 1994;91:2076–2080. [PubMed: 8134351]

Carson BS Sr, Wu Q, Tyler B, Sukay L, Raychaudhuri R, DiMeco F, Clatterbuck RE, Olivi A, Guarnieri M. New approach to tumor therapy for inoperable areas of the brain: chronic intraparenchymal drug delivery. J Neurooncol 2002;60:151–158. [PubMed: 12635662]

Eberling JL, Jagust WJ, Christine CW, Starr P, Larson P, Bankiewicz KS, Aminoff MJ. Results from a phase I safety trial of hAADC gene therapy for Parkinson disease. Neurology 2008;70:1980–1983. [PubMed: 18401019]

Fiandaca M, Eberling J, McKnight TR, Bringas J, Pivirotto P, Beyer J, Hadaczek P, Forsayeth J, Bowers WJ, Park J, Federoff HJ, Bankiewicz K. Real-Time MR Imaging of Adeno-Associated Viral Vector Delivery to the Primate Brain. Neuroimage. 2008a In Press.

Fiandaca MS, Forsayeth JR, Dickinson PJ, Bankiewicz KS. Image-guided convection-enhanced delivery platform in the treatment of neurological diseases. Neurotherapeutics 2008b;5:123–127. [PubMed: 18164491]

Forsayeth JR, Eberling JL, Sanftner LM, Zhen Z, Pivirotto P, Bringas J, Cunningham J, Bankiewicz KS. A Dose-Ranging Study of AAV-hAADC Therapy in Parkinsonian Monkeys. Mol Ther 2006;14:571–577. [PubMed: 16781894]

Gasmi M, Brandon EP, Herzog CD, Wilson A, Bishop KM, Hofer EK, Cunningham JJ, Printz MA, Kordower JH, Bartus RT. AAV2-mediated delivery of human neurturin to the rat nigrostriatal system: Long-term efficacy and tolerability of CERE-120 for Parkinson's disease. Neurobiol Dis 2007;27:67–76. [PubMed: 17532642]

Gill SS, Patel NK, Hotton GR, O'Sullivan K, McCarter R, Bunnage M, Brooks DJ, Svendsen CN, Heywood P. Direct brain infusion of glial cell line-derived neurotrophic factor in Parkinson disease. Nat Med 2003;9:589–595. [PubMed: 12669033]

Hadaczek P, Kohutnicka M, Krauze MT, Bringas J, Pivirotto P, Cunningham J, Bankiewicz K. Convection-enhanced delivery of adeno-associated virus type 2 (AAV2) into the striatum and transport of AAV2 within monkey brain. Hum Gene Ther 2006a;17:291–302. [PubMed: 16544978]

Hadaczek P, Yamashita Y, Mirek H, Tamas L, Bohn MC, Noble C, Park JW, Bankiewicz K. The "perivascular pump" driven by arterial pulsation is a powerful mechanism for the distribution of therapeutic molecules within the brain. Mol Ther 2006b;14:69–78. [PubMed: 16650807]

Herzog CD, Brown L, Gammon D, Kruegel B, Lin R, Wilson A, Bolton A, Printz M, Gasmi M, Bishop KM, Kordower JH, Bartus RT. Expression, bioactivity, and safety 1 year after adeno-associated viral vector type 2-mediated delivery of neurturin to the monkey nigrostriatal system support cere-120 for Parkinson's disease. Neurosurgery 2009;64:602–612. discussion 612–603. [PubMed: 19349823]

Herzog CD, Dass B, Holden JE, Stansell J 3rd, Gasmi M, Tuszynski MH, Bartus RT, Kordower JH. Striatal delivery of CERE-120, an AAV2 vector encoding human neurturin, enhances activity of the dopaminergic nigrostriatal system in aged monkeys. Mov Disord. 2007

Hornykiewicz O. Parkinson's disease and its chemotherapy. Biochem Pharmacol 1975;24:1061–1065. [PubMed: 239718]

Krauze MT, Forsayeth J, Park JW, Bankiewicz KS. Real-time imaging and quantification of brain delivery of liposomes. Pharm Res 2006;23:2493–2504. [PubMed: 16972184]

Krauze MT, McKnight TR, Yamashita Y, Bringas J, Noble CO, Saito R, Geletneky K, Forsayeth J, Berger MS, Jackson P, Park JW, Bankiewicz KS. Real-time visualization and characterization of liposomal delivery into the monkey brain by magnetic resonance imaging. Brain Res Brain Res Protoc 2005a;16:20–26. [PubMed: 16181805]

NIH-PA Author Manuscript

NIH-PA Author Manuscript

NIH-PA Author Manuscript

Krauze MT, Saito R, Noble C, Bringas J, Forsayeth J, McKnight TR, Park J, Bankiewicz KS. Effects of the perivascular space on convection-enhanced delivery of liposomes in primate putamen. Exp Neurol 2005b;196:104–111. [PubMed: 16109410]

Krauze MT, Saito R, Noble C, Tamas M, Bringas J, Park JW, Berger MS, Bankiewicz K. Reflux-free cannula for convection-enhanced high-speed delivery of therapeutic agents. J Neurosurg 2005c; 103:923–929. [PubMed: 16304999]

Kroll RA, Pagel MA, Muldoon LL, Roman-Goldstein S, Neuwelt EA. Increasing volume of distribution to the brain with interstitial infusion: dose, rather than convection, might be the most important factor. Neurosurgery 1996;38:746–752. discussion 752–744. [PubMed: 8692395]

Kunwar S. Convection enhanced delivery of IL13-PE38QQR for treatment of recurrent malignant glioma: presentation of interim findings from ongoing phase 1 studies. Acta Neurochir Suppl 2003;88:105–111. [PubMed: 14531568]

Lang AE, Gill S, Patel NK, Lozano A, Nutt JG, Penn R, Brooks DJ, Hotton G, Moro E, Heywood P, Brodsky MA, Burchiel K, Kelly P, Dalvi A, Scott B, Stacy M, Turner D, Wooten VG, Elias WJ, Laws ER, Dhawan V, Stoessl AJ, Matcham J, Coffey RJ, Traub M. Randomized controlled trial of intraputamenal glial cell line-derived neurotrophic factor infusion in Parkinson disease. Ann Neurol 2006;59:459–466. [PubMed: 16429411]

Larson PS, Richardson RM, Starr PA, Martin AJ. Magnetic resonance imaging of implanted deep brain stimulators: experience in a large series. Stereotact Funct Neurosurg 2008;86:92–100. [PubMed: 18073522]

Lonser RR, Corthesy ME, Morrison PF, Gogate N, Oldfield EH. Convection-enhanced selective excitotoxic ablation of the neurons of the globus pallidus internus for treatment of parkinsonism in nonhuman primates. J Neurosurg 1999;91:294–302. [PubMed: 10433318]

Lonser RR, Walbridge S, Garmestani K, Butman JA, Walters HA, Vortmeyer AO, Morrison PF, Brechbiel MW, Oldfield EH. Successful and safe perfusion of the primate brainstem: in vivo magnetic resonance imaging of macromolecular distribution during infusion. J Neurosurg 2002;97:905–913. [PubMed: 12405380]

Lonser RR, Warren KE, Butman JA, Quezado Z, Robison RA, Walbridge S, Schiffman R, Merrill M, Walker ML, Park DM, Croteau D, Brady RO, Oldfield EH. Real-time image-guided direct convective perfusion of intrinsic brainstem lesions. Technical note. J Neurosurg 2007;107:190–197. [PubMed: 17639894]

Mardor Y, Roth Y, Lidar Z, Jonas T, Pfeffer R, Maier SE, Faibel M, Nass D, Hadani M, Orenstein A, Cohen JS, Ram Z. Monitoring response to convection-enhanced taxol delivery in brain tumor patients using diffusion-weighted magnetic resonance imaging. Cancer Res 2001;61:4971–4973. [PubMed: 11431326]

Martin KJ, Neu CP, Hull ML. Quasi-steady-state displacement response of whole human cadaveric knees in a MRI scanner. J Biomech Eng 2009;131:081004. [PubMed: 19604016]

Murad GJ, Walbridge S, Morrison PF, Szerlip N, Butman JA, Oldfield EH, Lonser RR. Image-guided convection-enhanced delivery of gemcitabine to the brainstem. J Neurosurg 2007;106:351–356. [PubMed: 17410722]

Richardson RM, Larson PS, Bankiewicz KS. Gene and cell delivery to the degenerated striatum: status of preclinical efforts in primate models. Neurosurgery 2008;63:629–442. dicussion 642–624. [PubMed: 18981876]

Saito R, Bringas JR, McKnight TR, Wendland MF, Mamot C, Drummond DC, Kirpotin DB, Park JW, Berger MS, Bankiewicz KS. Distribution of liposomes into brain and rat brain tumor models by convection-enhanced delivery monitored with magnetic resonance imaging. Cancer Res 2004;64:2572–2579. [PubMed: 15059914]

Saito R, Krauze MT, Bringas JR, Noble C, McKnight TR, Jackson P, Wendland MF, Mamot C, Drummond DC, Kirpotin DB, Hong K, Berger MS, Park JW, Bankiewicz KS. Gadolinium-loaded liposomes allow for real-time magnetic resonance imaging of convection-enhanced delivery in the primate brain. Exp Neurol. 2005

Sampson JH, Akabani G, Friedman AH, Bigner D, Kunwar S, Berger MS, Bankiewicz KS. Comparison of intratumoral bolus injection and convection-enhanced delivery of radiolabeled antitenascin monoclonal antibodies. Neurosurg Focus 2006;20:E14. [PubMed: 16709019]

NIH-PA Author Manuscript

NIH-PA Author Manuscript

NIH-PA Author Manuscript

Sanftner LM, Sommer JM, Suzuki BM, Smith PH, Vijay S, Vargas JA, Forsayeth JR, Cunningham J, Bankiewicz KS, Kao H, Bernal J, Pierce GF, Johnson KW. AAV2-mediated gene delivery to monkey putamen: Evaluation of an infusion device and delivery parameters. Exp Neurol 2005;194:476–483. [PubMed: 16022872]

Varenika V, Dickenson P, Bringas J, LeCouteur R, Higgins R, Park JW, Fiandaca M, Berger MS, Sampson JH, Bankiewicz KS. Real-Time Imaging of CED in the Brain Permits Detection of Infusate Leakage. J Neurosurg 2008;109:874–880. [PubMed: 18976077]

Yin D, Valles FE, Fiandaca MS, Forsayeth J, Larson P, Starr P, Bankiewicz KS. Striatal volume differences between non-human and human primates. J Neurosci Methods 2009;176:200–205. [PubMed: 18809434]

NIH-PA Author Manuscript

NIH-PA Author Manuscript

NIH-PA Author Manuscript

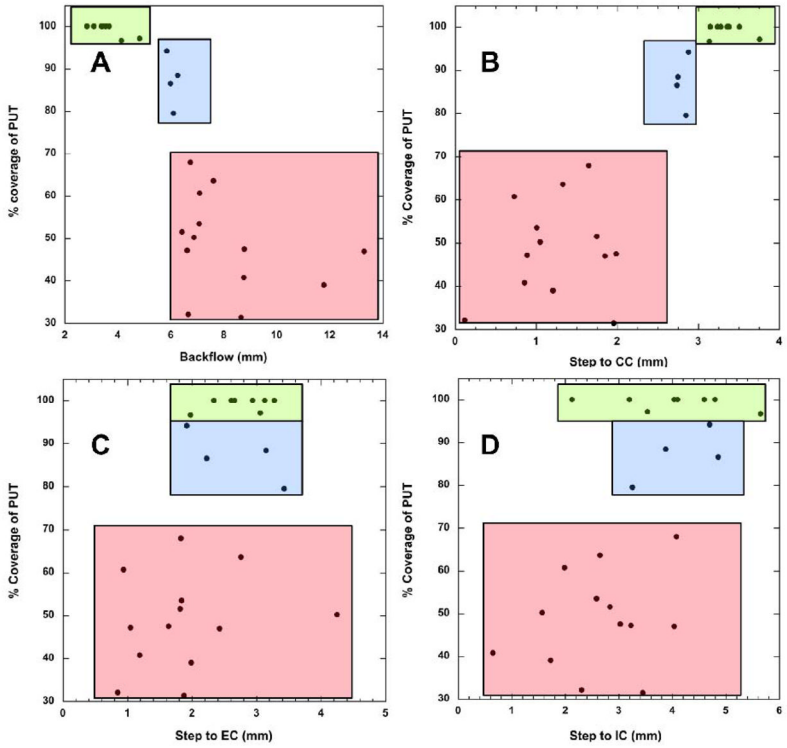

Figure 1.
Correlation of spatial coordinates and length of backflow with distribution of MRI tracer in the putamen

NIH-PA Author Manuscript

NIH-PA Author Manuscript

NIH-PA Author Manuscript

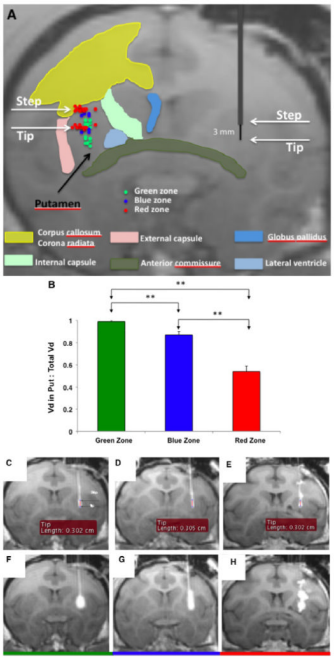

Figure 2. Stepped cannula placement in the putamen

(**A**) Schematic shows both step and tip portion of the cannula placement in green, blue and red zone for each case are shown. (**B**) Distribution is plotted as Vd in putamen vs. total Vd for each zone is shown ($p<0.01$). (**C**) Representative MR images showing distribution of Gadoteridol in the putamen for green, blue and red zones. Cannula placement and initial infusion are shown in panels C, D and E for each zone. Panels F, G and H show distribution of Gadoteridol in the brain after infusion into respective RGB zones. Note slight leakage into white matter tracts in G (blue) but pronounced leakage in H (red). Infusion into green zone (F) resulted in tracer distribution in putamen only.

NIH-PA Author Manuscript

NIH-PA Author Manuscript

NIH-PA Author Manuscript

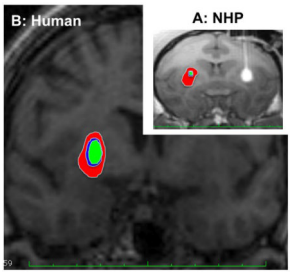

Figure 3.
RGB zones for step outlined in the putamen of NHP (A) and predicted for human putamen (B) based on the RGB parameters obtained in the NHP and compared on the same scale

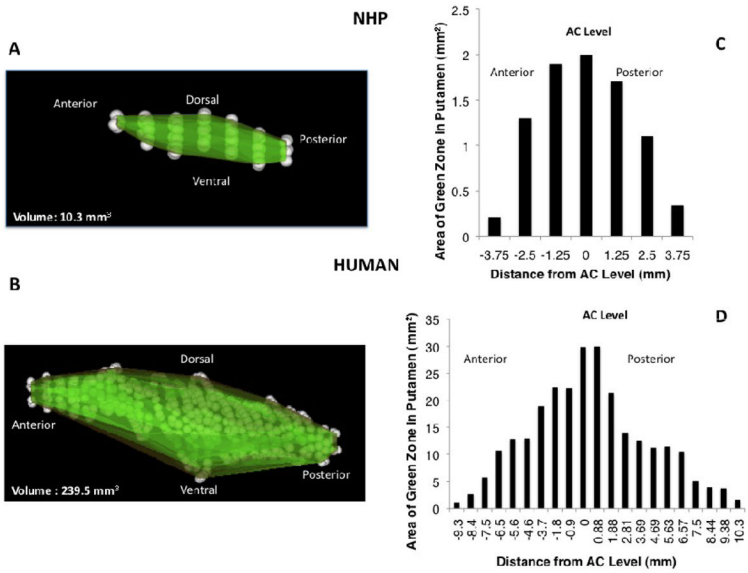

Figure 4. 3D reconstruction of green zone and representative volumes of "green zone" in NHP (A and C) and human putamen (B and D)

Area of green zone was defined from MR images as a volume at least 3 mm ventral to the CC, at least 6 mm away from the AC (3 mm from cannula tip to AC plus 3 mm of tip length) vertically, greater than 2.75 mm from EC laterally, and more than 3 mm from IC medially.

NIH-PA Author Manuscript NIH-PA Author Manuscript NIH-PA Author Manuscript

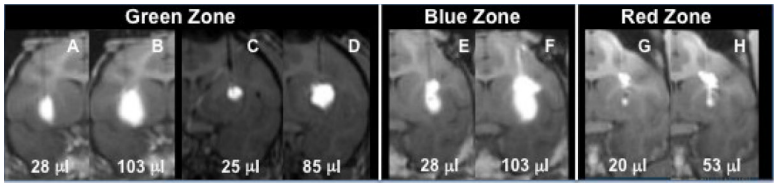

Figure 5.
Representative MR images showing distribution of Gadoteridol in the putamen and leakage into white matter tract at small and large infusion volume of MRI tracer

NIH-PA Author Manuscript
NIH-PA Author Manuscript
NIH-PA Author Manuscript

NIH-PA Author Manuscript NIH-PA Author Manuscript NIH-PA Author Manuscript

Table 1

Correlation of Spatial Coordinates with Reflux and Percent Coverage of Putamen
Measurement of distance from step to CC, IC and EC, length of backflow and percent distribution of MRI tracer in the putamen

Infusion	Step to CC (mm)	Step to IC (mm)	Step to EC (mm)	Reflux (mm)	% of PUT	Vd/Vi	Vd in put/Vd of leakage
1	3.38	4.8	2.94	3.54	100%	6.2	ND
2	3.24	4.04	3.28	3.1	100%	6.6	ND
3	3.76	3.54	3.06	4.83	97.1%	4.5	ND
4	3.14	5.65	1.98	4.14	96.6%	7.9	ND
5	3.36	4.1	2.66	3.42	100%	5.3	ND
6	3.51	4.6	2.34	3.68	100%	6.7	ND
7	3.15	2.13	2.61	2.84	100%	9.1	ND
8	3.28	3.2	3.13	3.39	100%	7.0	ND
9	2.88	4.7	1.92	5.85	94.2%	4.0	16.30
10	2.85	3.26	3.43	6.1	79.5%	5.1	3.88
11	2.74	4.86	2.23	5.99	86.5%	4.5	6.43
12	2.75	3.88	3.15	6.26	88.4%	4.8	7.62
13	1.65	4.08	1.83	6.74	67.9%	4.2	2.11
14	1.01	2.59	1.84	7.08	53.5%	3.1	1.15
15	1.75	2.84	1.82	6.43	51.5%	0.9	1.07
16	1.85	4.04	2.43	13.29	47.0%	3.8	0.89
17	1.96	3.45	1.88	8.65	31.4%	2.5	0.46
18	0.12	2.31	0.85	6.66	32.1%	0.6	0.47
19	0.86	0.65	1.19	8.76	40.8%	2.2	0.69
20	0.73	1.99	0.94	7.09	60.7%	2.8	1.54
21	1.33	2.65	2.76	7.61	63.6%	3.1	1.75
22	1.99	3.03	1.64	8.78	47.5%	3.0	0.91
23	1.21	1.73	1.99	11.78	39.0%	4.9	0.64
24	0.89	3.23	1.05	6.62	47.2%	2.4	0.89
25	1.05	1.57	4.25	6.88	50.2%	4.4	1.01

NIH-PA Author Manuscript NIH-PA Author Manuscript NIH-PA Author Manuscript

Spatial coordinates correlated with length of backflow and percent of containment of tracer within the putamen. The ratio of Vd in PUT to Vd of leakage was obtained by dividing the volume of distribution of tracer in the putamen by the volume of leakage of tracer into white matter tract. CC, corpus callosum; IC, internal capsule; EC, external capsule; PUT, putamen; and Vd, volume of distribution.